Application of Computational Fluid Dynamics in Simulation and Optimization of a Fluidized Sugar Bed Dryer

NABASIRYE SUSAN[1], RICHARD O. AWICHI[3], STEPHEN KADEDESYA[1],
ANSELM O. OYEM[1,2,*]
[1]Department of Mathematics,
Busitema University,
UGANDA

[2]Department of Mathematics,
Federal University Lokoja,
NIGERIA

[3]Department of Mathematics and Statistics,
Kyambogo University,
UGANDA

Corresponding Author

Abstract: - The application of computational fluid dynamics (CFD) in the design of industrial thermal process equipment is of great importance. Food drying is an important process in the sugar processing industry as it helps in the easy of transportation and storage, and also increases the life span of food. In this study a two-dimensional (2D) fluidized bed dryer is designed in the Blockmesh Dict file an application in the OpenFOAM with dimensions height 0.8m and diameter $0.5m$. The Navier-Stokes equations were solved to provide the flow variation that occurs inside the fluidized bed dryer in terms of temperature and velocity. For optimization of results, Taguchi analysis was considered and the results show that at a very low temperature below 50^0C, the sugar drying process is slow leading to much time being spent for effective sugar drying. Also an increase in flow velocity results in a faster drying rate of sugar granules. During the optimization of the performance of the fluidized sugar bed dryer, the percentage contribution of sugar granules diameter is more significant than other factors and it was also noted that pressure has less significance on the drying process within the fluidized bed.

Key-Words: - CFD, OpenFOAM, Fluidization, ANOVA, Taguchi technique, 2D.

Received: June 3, 2023. Revised: October 27, 2023. Accepted: December 18, 2023. Published: December 31, 2023.

1 Introduction

Over the years computational fluid dynamics (CFD) has become a beacon of research in several aspects of human endeavors, say, industrial applications and processes like, drying of food and beverages, pharmaceutical drug production; environmental processes in wastewater sludge, storages, transportation. Technological advancements and the current high demands in consumption and production, have given room to the exploration and usage of various innovative drying techniques and utilization of drying equipment for productions, ranging from applications in chemical, biochemical, pharmaceutical, and agricultural sectors to drying of various materials for a variety of industrial and technological applications, making, [1], to comprehensively, review the application of CFD in both industrial and lab-based drying applications. It was observed that CFD can be used as a tool to predict hydrodynamic heat and mass transfer mechanisms occurring in the processes. This made, [2], look into improving the drying performance of parchment coffee due to the newly redesigned drying chamber. Furthermore, conducting a simulation using CFD helped them attain a better unit's dryer air behavior, notable drying times reduction, and improved air distribution. The pore structure distribution and coupled heat and moisture transfer during the drying process of grains using a fixed-bed corn drying process were looked into by [3].

Sugar bed dying in any processing industry is of great importance because of the preservative

procedures because of the notion that it saves time and money, [4]. Globally, various methods have been put in place to help in the sugar drying process like the vibrative dryer, rotary drum dryer, and the fluidized dryer, [5]. But, [6], gave a review of the common dilemma plaguing spray drying modelling using a plug-flow simulation approach to the counter-current spray drying process with the CFD technique. [7], looked into the development of a fluidized bed dryer for drying a sago bagasse. They observed that high temperature and air feed velocity results in a rapid drying rate with the advantage of reducing the power energy and cost supply.

A fluidized bed dryer (FBD) is one of the most regularly used and established drying methods for wet solid particles due to its high production rate of heat and mass transfer which ensures a considerably faster and homogeneous drying process. The advantages of FBD are huge as a result of its experimental or simulation successes recorded. Some of these advantages include providing a large contact area between solid and air, a high solid mixing level, adequate heat and mass transfer between solid and air, and providing better temperature and operational control along the drying process. In a fluidized bed dryer, the hot gas is passed through the bed of solids at a velocity sufficient to keep the bed in a fluidized state where, mixing and heat transfer are very rapid and the equipment works on a principle of fluidization of the feed materials as shown in Figure 1, [8], [9].

CFD techniques are used to solve complex engineering problems and their applications, fluid flow, heat, and mass transfer problems. Hence, its application and simulation use cannot be over-emphasised especially in the drying processes. The use of CFD in numerical analysis has shown good results in solving problems of fluid flow with heat and mass transfer, [10] and this has attracted many researchers due to its industrial, environmental, and scientific applications, [11], [12], [13], [14], [15], [16], [17], [18]. [19], analyzed the process of using CFD modeling with the developed three-dimensional FBD model while, [20], studied a bubbling flow in a 2D pulsed fluidized bed dryer using the Eulerian approach, and their results showed that pressure changes inside the bed, was due to the formation of air bubbles at minimal frequency pulsating inlet flow causing intermittent fluidized state. [21], investigated the effect of operating parameters of sucrose fluid bed drying powder quality and drying time to optimize the production of sucrose powder. They observed that gas flow and sugar particle size had significant effects on the quality of the sugar dried with 99.9699% drying time.

The effect of increasing the air inlet size and the bed thickness on the thermal behavior of the dryer was studied by [22] and their study showed that air inlet size is proportional to the moisture extraction and increasing the bed dryer prolongs the drying period. Then, the airflow in a mixed-flow dryer was studied by [23], to determine its influence on air duct size, results indicated that small ducts yield higher velocity rates.

Since clumping and discoloration of sugar as a result of the sugar not properly being dried is one of the key problems faced in sugar manufacturing industries, this has led to poor quality and low value of sugar produced and unsafe for storage. Fluidized bed drying is one of the popular methods used for drying sugar in industries, the drying mechanism within the dryer depends on different factors like air temperature, pressure, air velocity, and bed thickness among others, and the combined effects are not yet explored adequately.

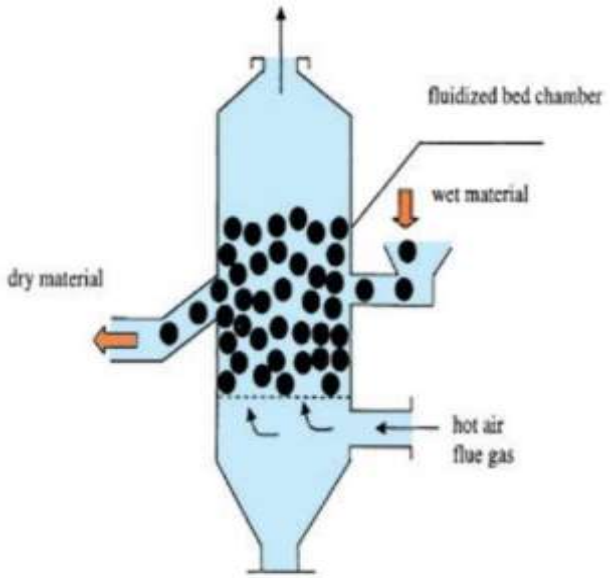

Fig. 1: Concept of Fluidized bed drying

Hence, in the current study an OpenFOAM software in CFD is applied and simulated to establish the effect of air velocity, pressure, and drying air temperature on the sugar drying process within a fluidized bed dryer as well as to optimize the performance of a fluidized sugar bed dryer and validate the optimum process parameters for sugar drying.

2 Problem Formulation

A fluidized sugar bed dryer 2D geometry was developed using the blockMesh in OpenFOAM 7 software, meshed, and the Navier-Stokes equations discretized. A Newtonian fluid flow in the drying chamber is incompressible, with constant physical and chemical properties for airflow in the bed dryer and for turbulence considered.

Based on the assumption that the governing equations conserve all laws for each control volume of the domain, the fluid flow and heat transfer of the governing continuity, momentum and energy equations are given below:

$$\nabla.\vec{V} = 0, \tag{1}$$

where V is the velocity vector of airflow which depends on the coordinates x, y.

and,

$$\frac{\partial(\rho\vec{V})}{\partial t} + \nabla\cdot(\rho\vec{V}\,\vec{V}) = -\nabla p + \mu\nabla^2\vec{V} + \rho g. \tag{2}$$

Where, ρ is the density of the fluid, $\vec{V}$ is the velocity component, p is the fluid pressure, μ is dynamic viscosity and g is acceleration due to gravity.

In modeling of thermal processes, it requires that the energy equation governing the heat transfer within a fluid system is solved and this equation is written as:

$$\frac{\partial(\rho C_a T)}{\partial t} + \nabla\cdot(\rho\vec{V}C_a T) = \lambda\nabla^2 T + S_T\,. \tag{3}$$

Where, C_a is the specific heat capacity of hot air T is Temperature, λ is thermal conductivity and S_T is the thermal sink or source. The Fourier equation governs heat transfer in an isotropic solid given by [24], [25].

$$\frac{\partial(\rho C_a T)}{\partial t} = \lambda\nabla^2 T + S_T\,. \tag{4}$$

The convective mixing term for temperature, is incorporated in Eq. (3). For a conjugate heat transfer situation where evaporation at the sugar surface is considered, and heat transfer coefficient is known, the boundary condition for Eq. (4) is given by:

$$h(T_f - T_s) + \varepsilon_f\sigma(T_f^4 - T_s^4) = -\lambda\frac{\partial T}{\partial n} - \alpha_v\cdot N_u\,. \tag{5}$$

Where T_f is temperature of the bulk fluid, T_s is temperature of surface, α_v is water molar latent heat of vaporization ($Jmol^{-1}$), ε_f is the emission factor coefficient, σ is the Stefan Boltzmann constant and N_u is Nusselt number.

The heat transported by radiation and convection from hot air to sugar, raises the sample temperature and drives towards evaporating the free water at the surface, [26]. Solution of Eq. (5) can be used on the sugar surface to calculate the local heat transfer coefficients, [27] below:

$$h = \frac{\left[-\lambda\frac{\partial T}{\partial n}\right]_{surface}}{T_f - T_s}\,. \tag{6}$$

Since, sugar drying is a thermal process associated with turbulent motion (high flow rates and heat transfer interactions in the drying chambers), consider the standard $k-\epsilon$ turbulence model, which is a two-equation model making a closure to Reynolds Averaged Navier-Stokes (RANS) to model the fluid flow phenomenon in the fluidized bed drying chamber. The RANS equations play an important role in modelling both steady-state and turbulent flow phenomena containing two transport equations; turbulent kinetic energy k and dissipation rate of turbulent kinetic energy ϵ. For the $k-\epsilon$ turbulence model, the turbulent viscosity μ_t is given as:

$$u_t = \rho C_\mu\frac{k^2}{\epsilon} \tag{7}$$

showing that turbulence viscosity μ_t, depends on the kinetic energy k and its dissipation rate ϵ.

The turbulence kinetic energy transport equation is expressed as:

$$\frac{\partial k}{\partial t} + \vec{V}(\nabla k) = P_k - \epsilon + \nabla\cdot\left(\frac{v_t}{\sigma_k}\nabla k\right) + v\nabla\cdot(\nabla k) \tag{8}$$

with dissipation rate of turbulence kinetic energy given as:

$$\frac{\partial\epsilon}{\partial t} + \vec{V}(\nabla\epsilon) = -C_{\epsilon1}\frac{\epsilon^2}{k}P_k - C_{\epsilon2}\frac{\epsilon^2}{k} + \nabla\cdot\left(\frac{v_t}{\sigma_\epsilon}\nabla\epsilon\right) + v\nabla\cdot(\nabla\epsilon)\,. \tag{9}$$

Where, P_k is the production rate of turbulent kinetic energy per unit mass and $C_{\epsilon1}$, $C_{\epsilon2}$, σ_k, σ_ϵ, C_μ are model constants, [28], with coefficient values as shown in Table 1. Solving Eqs. (8) and (9) numerically, yields the turbulence kinetic energy and the kinetic dissipation rate respectively.

Table 1. The $k-\epsilon$ turbulence model coefficients.

Constant	C_μ	$C_{\epsilon 1}$	$C_{\epsilon 2}$	σ_k	σ_ϵ
Value	0.09	1.44	1.92	1.00	1.30

Performing numerical simulation, the geometry for the computational domain of the 2D fluidized bed dryer as developed using the inbuilt Blockmesh file in the system directory of OpenFOAM software is shown in Figure 2. A cylindrical fluidized bed dryer of bed height $0.8m$ and internal diameter $0.5m$ is considered to determine the sugar profile of the sugar bed dryer at varying times establishing the effect of varying air velocity, temperature, and pressure on bed height of drying sugar.

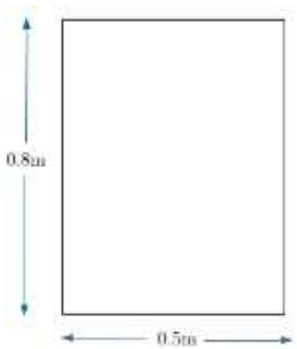

Fig. 2: Geometry of a 2D fluidized bed dryer

Using the blockMesh and snappyHexMesh utilities in OpenFOAM 7.0., the geometry mesh is presented in Figure 3. The blockMesh utility generates elementary meshes of blocks with hexahedral cells. A sizable background mesh was created from the OpenFOAM Blockmesh dictionary file which is found in the system directory and runs in paraFoam ParaView. Since the simulation is transient, smaller sized meshes are considered in OpenFOAM such that the Courant number is close to 1 for accuracy and numerical stability.

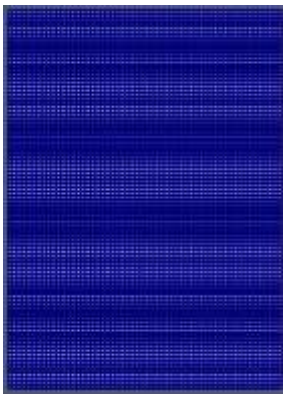

Fig. 3: A sizable computational mesh of the fluidized bed dryer

In this paper, initial inlet air velocity of $1.3ms^{-1}$, air pressure of $101350Pa$ and air temperature of $400K$ are considered in the simulation because they are ideal ones which can move the fluidized sugar during the drying process while the boundary conditions in OpenFOAM used in the simulation is shown in Table 2.

Table 2. Boundary conditions for simulation in OpenFOAM, [14]

Boundary field	Inlet	Outlet
Air velocity	Fixed value	Pressure Inlet Outlet value
Air temperature	Total temperature	Total temperature
Air pressure	Fixed flux pressure	Fixed value

3 Results and Discussion

For simulation of the mass transfer reaction of the hot air (gas) phase and moist sugar phase in the fluidized bed dryer, a reacting two-phase EulerFoam, a multiphase solver in OpenFOAM 7.0 was used. Mass transfer involves the transport of species among phases through diffusion (physical) and, or chemical reactions in a special unit operation (reactor), allowing such a process to take place. A chemical reaction is used to haste up the mass transfer rate, whenever species of different chemical potentials are brought into contact, with hot air and moist sugar. According to [28], to capture the interphase between the two phases, reacting two-phase EulerFoam uses the volume of fluid (VOF) method. To know where the interphase is:

$$\frac{\partial \alpha}{\partial t} + \nabla \cdot (\alpha \bar{V}) = 0 \qquad (10)$$

is worked out. Where, $\bar{V}$ is the mean velocity and α is the volume fraction within a cell. The model employs volume fraction α to denote the individual phases. The volume fraction $\alpha = 1$ represents a computational cell that is completely filled with water and for $\alpha = 0$ represents a cell completely filled with air. The liquid-gas interface arises within mesh cells where α takes on values between 0 and 1.

The solver works out both the continuity and Naiver-Stokes equations for two incompressible, isothermal, immiscible, transient, and turbulent fluids where, the material properties such as the density, viscosity, and specific heat capacity are constant in the region filled by one of the two fluids except at the interphase, [29]. Visual and graphical

results were then generated using ParaView as seen in simulated sugar volume fraction profiles of 2D bed at $t = 0, 0.5, 1$ and 1.5 seconds and displayed in Figure 4, Figure 5, Figure 6, Figure 7 and Figure 8.

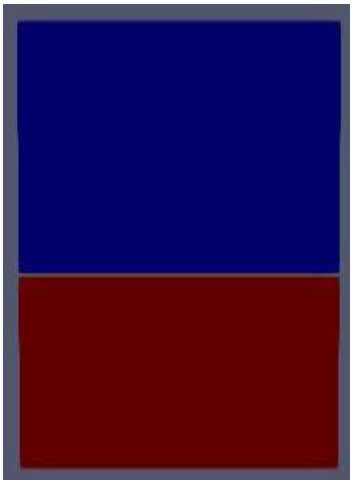

Fig. 4: Sugar at t = 0s

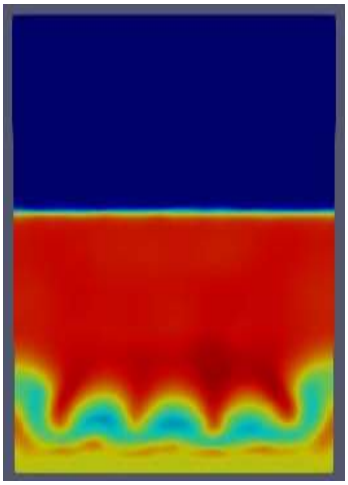

Fig. 5: Sugar at t = 0.5s

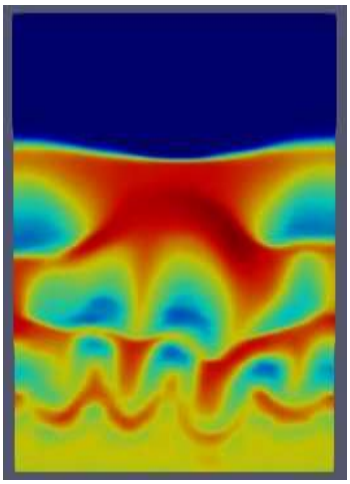

Fig. 6: Sugar at t = 1s

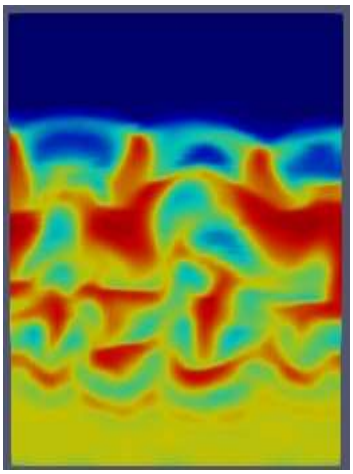

Fig. 7: Sugar at $t = 1.5s$

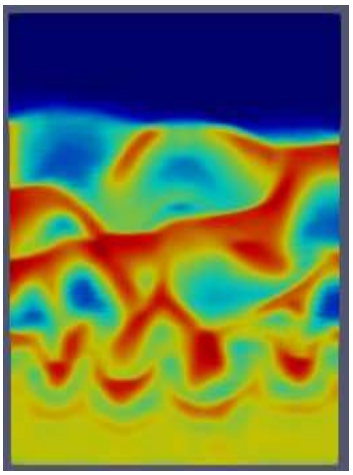

Fig. 8: Sugar at $t = 2s$

From Figure 4 and Figure 5, sugar is represented by the red colour, while the blue color represents the gas-phase. It is observed that at $t = 0\ sec$, the sugar granules are static (not yet fluidized) as the fluidization process begins when a particular inlet air velocity threshold value exceeds $t = 0.5\ secs$ to maximum fluidization at $t = 2s$. Maximum fluidization occurs when all the sugar granules are in a fluidized state. After the moisture content in the sugar reached 0% wet basis, turbulent fluidization was realized and the sugar drying process was considered complete. At time $t = 0s$, the wet sugar granules are introduced in the bed dryer, and there is no drying hot air introduced, so the sugar granules appear to be stationary. Furthermore, at $t = 0.5s$, hot air starts entering the fluidized bed dryer through the inlet at the bottom, and is seen raising the sugar slowly since the sugar is so moist 10%. Then, $t = 1s$, the rate of hot air entering the fluidized bed dryer is seen to increase moving the moist sugar granules to a higher height within the fluidized bed dryer. Though, the fluidization process of the sugar granules is seen to start slowly within

the bed but, at time $t = 1.5s$, as more hot air continuously enters into the bed dryer with increasing velocity, sugar granules get into more fluidization and they move with turbulent motion within the bed dryer causing the sugar to dry in a homogeneous way. At time $t = 2s$, the sugar goes on drying as the moisture content reduces and it moves more vigorously in turbulent motion in the fluidized form as a result of more drying hot air entering the bed with a higher velocity

The air which is initially entering at $1.03ms^{-1}$, decreases to $0.9ms^{-1}$ at a fluid bed height of $0m$. This effect is due to the drag force of sugar particles on each particle as sugar remains in close configuration. The velocity of air decreases further to $0.75ms^{-1}$ to a height of $0.11m$. The velocity of air further decreases because the air continues to absorb moisture from the sugar making it move to a height of $0.11m$. The velocity is then seen to increase drastically from $0.75ms^{-1}$ at a height of $0.20m$ to $1.3ms^{-1}$ at a height of $0.25m$. This makes the particles move away from each other and become suspended within the fluidized bed dryer, causing the bed to expand. As the air velocity increases, the wall shear stresses increase and the pressure begins to increase, hence pressure increases with gas velocity. Between the height of $0.2m$ to $0.65m$, there is an increase in the drying rate of the sugar and hot air hence decrease in the moisture content as illustrated in the Figure 9.

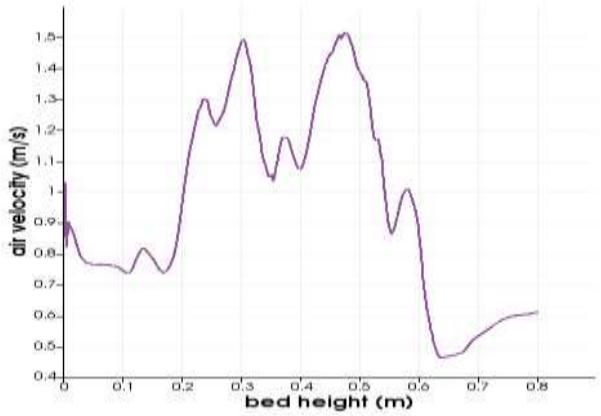

Fig. 9: Gas velocity distribution within a fluidized bed chamber

The pressure within the bed is initially at $101350Pa$ at a height of $0.00m$ and the pressure significantly decreases from $101350Pa$ to $98600Pa$ at a height of $0.20m$. The decrease is due to the sugar having more moisture thus being dominated by inter-particle frictional forces. Then, pressure increases from $98600Pa$ to $100000Pa$ at a height of $0.35m$. The increase is due to the expansion of the bed and decrease in the amount of sugar moisture which makes the sugar granules move upwards from the bottom of the bed as a result of being fluidized (Figure 10).

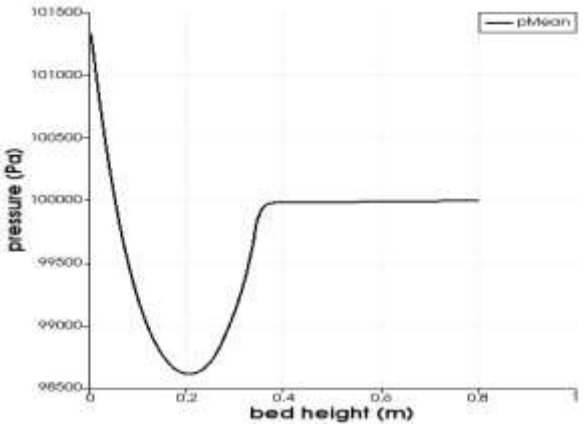

Fig. 10: Pressure distribution within a fluidized bed chamber

The temperature at which air enters the bed was $400K$ and the temperature decreased to $285k$ at a bed height of $0.00m$. The decrease is caused by a lot of moisture in the sugar granules which absorbs the heat of the hot drying air causing a drastic decrease in temperature. The temperature of $285K$ is maintained from a bed height of $0.01m$ to $0.40m$ and remains constant within that range of bed height due to the uniform mixture of the hot air and moist sugar. Subsequently, temperature of air increases from $285K$ at a height of $0.35m$ to $295K$ at a bed height of $0.40m$. This is due to more hot air entering the bed with reduced moisture in the sugar. The $295K$ temperature is maintained from a bed height of $0.40m$ to a bed height of $0.78m$ and this is attributed to the homogeneous drying of sugar granules to moist content of about 1%, as shown in Figure 11.

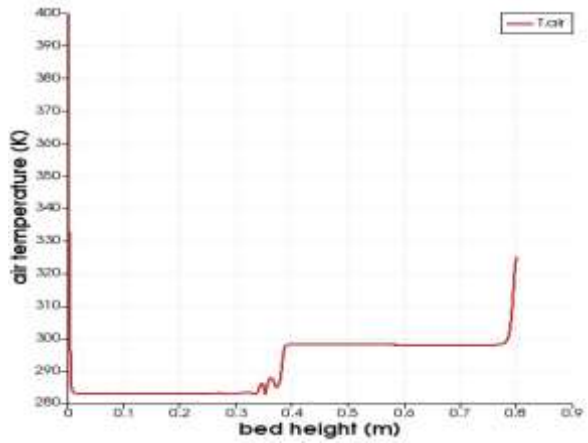

Fig. 11: A graph showing air temperature distribution within a fluidized bed chamber

3.1 Optimization of a Fluidized Sugar Bed Dryer Performance

In optimizing the performance of fluidized sugar bed dryers, a technique that handles large number of samples with fewer trials is used. Using the Taguchi technique (T), the results were analyzed by ranking the factors (Table 3) that affect the energy utilization ratio in the fluidized sugar bed dryer. The Taguchi L9 orthogonal array of the simulations is shown in Table 4.

The level of interaction in Table 5, represents the interaction between factors listed in Table 3, where, both inlet air temperature and sugar granule diameter have the greatest interaction. Inlet air temperature-inlet air velocity and sugar granule diameter-inlet air velocity are the pairs whose interactions are significant though to a lesser extent.

Using ANOVA analyses, the parameters of the response by the decomposition of the total variation and its appropriate components by measuring their relative effects were determined (Table 6).

From Table 6, the sugar granule diameter factor (B) contributed the highest percentage to the factor effects. Based on Taguchi technique, the expected energy utilization ratio, which is the sum of the total contribution from all factors and the grand average value is 0.273 in Table 8. The difference between the grand average value and the average effect of each factor corresponding to its optimum level is the contribution of each factor from Table 7, [30].

In the verification test phase, an additional simulation was done using the optimum conditions and the results obtained were compared with the expected results at optimum conditions. The confidence interval of the energy utilization ratio for this extra simulation was ± 0.021 and it was within the 95% confidence level of the predicted optimal values, which meant that the prediction by the Taguchi method is reliable (Table 8)

Table 3. The various parameters selected and their respective levels.

Factors	Level 1	Level 2	Level 3
A: Inlet air temperature $(0C)$	40	60	90
B: Sugar granule diameter (mm)	0.04	0.06	0.08
C: Inlet air velocity (ms^{-1})	2.5	4	6

Table 4. Taguchi L9 orthogonal array design

Simulation number	A	B	C
1	1	1	1
2	1	2	2
3	1	3	3
4	2	1	2
5	2	2	3
6	2	3	1
7	3	1	3
8	3	2	1
9	3	3	2

Table 5. Interaction between factors

Interaction factor pairs	Interaction severity index
A – B	28.05
A – C	21.02
B – C	11.34

Table 6. ANOVA Results

Factor	Degree of freedom (DOF)	Sum of squares (S)	Variance (V)	F-ratio (F)	Pure sum (S)	Percent, P (%)
A: Inlet air temperature (K)	2	0.002	0.001	4.843	0.002	20.13
B: Sugar granule diameter (m)	2	0.012	0.006	18.712	0.018	54.114
C: Inlet air velocity (m/s)	2	0.003	0.001	3.011	0.001	7.61
Other / error	2	0.004				18.146
Total	8	0.021				100

Table 7. Energy utilization ratio in Taguchi tests

Simulation number	Energy utilization ratio
1	0.040
2	0.028
3	0.012
4	0.161
5	0.120
6	0.101
7	0.231
8	0.141
9	0.196

Table 8. Estimation of the optimum condition (maximum energy utilization ratio)

Factor	Level	Contribution
A: Inlet air temperature (K)	3	0.071
B: Sugar granule diameter (mm)	1	0.042
C: Inlet air velocity (ms^{-1})	3	0.020
Total contribution from all factors		0.133
Current grand average of performance		0.140
Expected result at optimum condition		0.273

4 Conclusion

Fluidized bed dryer simulation using Computational Fluid Dynamics (CFD) was considered to investigate the effect of different parameters such as inlet air temperature, inlet air velocity and sugar granule diameter on energy utilization ratio at three levels using Taguchi technique. The data and results were obtained basically through simulation using an OpenFOAM application called blockMesh Dict file to fluidized bed dryer with the flow variables being velocity and temperature, and the optimized results were done using Taguchi analysis. From the analysis, the following conclusions are made:

1. Very low temperature below 50^0C results in a slower sugar drying process leading to much time being spent on the effective sugar drying process.
2. Pressure build-up within the fluidized sugar bed dryer increases with time as the hot air is being pumped into the bed and the sugar granules tend to be more spaced as the moisture content is lost.
3. The velocity of the air within the fluidized bed dryer as well as the velocity of the sugar granules generally increases with time specifically, after the minimum fluidization velocity is obtained.
4. The percentage contribution of the sugar granule diameter is more significant than the other factors and the pair inlet air temperature-sugar granule diameter has the maximum interaction with each other, with the pair sugar granule diameter - inlet air velocity having the least/minimum interaction on each other.
5. Moderate the temperature of the drying air from 60^0C to 90^0C ensure effective drying without melting the sugar granules as well as not consuming a lot of time and energy during the drying process.

The constant use of CFD in fluidized bed drying processes is becoming complex, and as such, further research can be carried out in areas of improved grid convergence, obtaining the thermophysical parameter effects on the fluid flow, and exploration of a different application to provide room for comparison, improved simulation and obtaining the error analysis.

Acknowledgement:
The authors hereby acknowledge the effort put forth by the reviewers and editorial board toward a successful manuscript.

References:

[1] Tarek, J. Jamaleddine and Madhumita B. Ray, Application of computational fluid dynamics for simulation of drying processes: a review, *Drying Technology*, Vol. 28, No. 2, 2010, pp. 120-154, https://doi.org/10.1080/07373930903517458.

[2] Eduado Duque-Dussán, and Jan Banout, Improving the drying performance of parchment coffee due to the newly redesigned drying chamber, *Journal of Food Process Engineering*, Vol. 45, No. 12, 2022, e14161, https://doi.org/10.1111/jfpe.14161.

[3] Liu W., Chen G., Zheng D., Ge M., and Liu C., Effects of the broken kernel on heat and moisture transfer in fixed-bed corn drying using particle-resolved cfd model, *Agriculture*, Vol.13, No. 8, 2023, 1470, https://doi.org/10.3390/agriculture13081470.

[4] Narjes Malekjani, and Seid Mahdi Jafari, Simulation of food drying processes by computational fluid dynamics: recent advances and approaches, *Trends in Food Science and Technology*, Vol. 78, 2018, pp. 206–223, https://doi.org/10.1016/j.tifs.2018.06.006.

[5] Junpeng Yi, Xin Li, Jian He, and Xu Duan, Drying efficiency and product quality of biomass drying: a review, *Drying Technology*, Vol.38, No. 15, 2020, pp. 2039–2054, https://doi.org/10.1080/07373937.2019.1628772.

[6] Ramin Razmi, Hasan Jubaer, Michal Krempski-Smejda, Maciej Jaskulski, Jie Xiao, Xiao Dong Chen, and Meng Wai Woo, Recent initiatives in effective modeling of a spray drying, *Drying Technology*, Vol.39, No. 11, 2021, pp. 1614-1647,

https://doi.org/10.1080/07373937.2021.1902344.

[7] Nur Tantiyani Ali Othman, and Ivan Adler Harry, Development of a fluidized bed dryer of a sago bagasse, *Pertanika Journal of Science and Technology*, Vol.29, No. 3, 2021, pp. 1831-1845, https://doi.org/10.47836/pjst.29.3.13

[8] Sivakumar, R., Saravanan, R., Perumal, A.E. and Iniyan, S., Fluidized bed drying of some agro products, *Renewable and Sustainable Energy Reviews*, Vol.61, 2016, pp. 280-301, https://doi.org/10.1016/j.rser.2016.04.014.

[9] Jinlai Zhang, Yanmei Meng, Hui Wang, Tao Yao, Shuangshuang Yu, and Ji Chen, Optimization design of cane sugar evaporative crystallizer based on orthogonal test and computation fluid dynamics, *Journal of Food Process Engineering*, Vol.43, No. 4, 2020, e13355. https://doi.org/10.1111/jfpe.13355

[10] Esemu Joseph Noah, Verdiana Grace Masanja, Hasifa Nampala, Joseph Ddumba Lwanyaga, Richard O. Awichi, and Twaibu Semwogerere, An application of computational fluid dynamics to optimize municipal sewage networks: a case of Tororo municipality, Eastern Uganda, 2020, Journal of Advances in Mathematics, Vol. 18 (2020) ISSN: 2347-1921, https://doi.org/10.24297/jam.v18i0.8345.

[11] Arumuganathan, T., Manikantan, M.R., Ramanathan, M., Rai, R.D, Indurani, C., and Karthiayani, A., Effect of diffusion channel storage on some physical properties of button mushroom (*Agaricus bisporus*) and shelf-life extension, *Proceedings of the National Academy of Sciences, India Section B: Biological Sciences*, Vol.83, 2017, pp. 705-718, https://doi.org/10.1007/s40011-015-0628-4.

[12] Winifred N. Mutuku, and Anselm O. Oyem, Casson Fluid of a Stagnation-Point Flow (SPF) towards a vertically Stretching/Shrinking Sheet, *FUDMA Journal of Sciences (FJS),* Vol. 5, No. 1, 2021, pp. 16-26. https://doi.org/10.33003/fjs-2021-0501-508

[13] Jalil, Nejadi and Ali Mohammad Nikbakht, Numerical simulation of corn drying in a hybrid fluidized bed-infrared dryer, *Journal of Food Process Engineering*, Vol. 40, No.2, 2017, e12373, https://doi.org/10.1111/jfpe.12373.

[14] Tantiyani N.A. Othman, Zaidi A.M. Din and Sobri M.M. Taakrif, Simulation on drying of sago bagasse in a fluidized bed dryer, *Journal of Engineering Science and Technology*, Vol. 15, No. 4, 2020, pp. 2507-2521.

[15] Oyem O. Anselm, Magnetic Effects on Laminar Convective Heat and Mass Transfer over a Vertical Plate with Arrhenius Kinetics, *Islamic University Multidisciplinary Journal*, Vol. 6, No. 4, 2019, pp. 195–204.

[16] Nico Jurtz, Urvashi Srivastava, Alireza Attari Moghaddam and Mattias Kraume, Particle-resolved computational fluid dynamics as the basis for thermal process intensification of fixed-bed reactors on multiple scales, *Energies*, Vol. 14, No. 10, 2021, 2913, https://doi.org/10.3390/en14102913.

[17] Onyekachukwu Anselm Oyem, Adeola John Omowaye, and Olubode Kolade Koriko, Combined Effects of Viscous Dissipation and Magnetic Field on MHD Free Convection Flow with Thermal Conductivity over a Vertical Plate, *Daffodil International University Journal of Science and Technology,* Vol. 10, No. 1-2, 2015, pp. 21–26.

[18] Zhenya Duan, Zhuang Zhang, Jingtao Wang, Xing Cao and Junmei Zhang, Thermal performance of structured packed bed with encapsulated phase change materials, *International Journal of Heat and Mass* Transfer, Vol. 158, 2020, 120066, https://doi.org/10.1016/j.ijheatmasstransfer.2020.120066.

[19] Abdul Mu'im Abdul Nasir, Masli Irwan Rosli, Mohd Sobri Takrif, Nur Tantiyani Ali Othman, and Vinotharan Ravichandar, Computational fluid dynamics simulation of fluidized bed dryer for sago pitch waste drying process, *Jurnal Kejuruteraan*, Vol.33, No. 2, 2021, pp. 239-248, https://doi.org/10.17576/jkukm-2021-33(2)-09

[20] Zhanyong Li, Weiguang Su, Zhonghua Wu, Ruifang Wang, and Mujumdar, A.S., Investigation of flow behaviours and bubble characteristics of a pulse fluidized bed via CFD modeling, *Drying Technology*, Vol.28, No. 1, 2009, pp. 78-93, https://doi.org/10.1080/07373930903430785.

[21] Amira Touil, and Ahiem Haj Ammar, Experimental design approach for optimization of sucrose fluid bed drying process conditions, *Global Journal of Pharmacy & Pharmaceutical Sciences*, Vol.4, No. 1, 2017, pp. 001-007, https://doi.org/10.19080/GJPPA.2017.04.555628.

[22] Khaldi, S., Korti, A.N. and Abboudi, S., Applying CFD for studying the dynamic and thermal behavior of an indirect solar dryer: parametric analysis, *Mechanics and Mechanical Engineering*, Vol.22, No. 1, 2018, pp. 253–272, https://doi.org/10.2478/mme-2018-0022.

[23] Zhen Li, Shunqi Mei, Nikolay Andrianor, and Lingxue Kong, Simulation of air flow in a mixed-flow grain dryer, UDC 677, 2015, pp. 258–264.

[24] Tomás Norton, Brijesh Tiwari and Da Wen Sun, Computational fluid dynamics in the design and analysis of thermal processes: a review of recent advances, *Critical Reviews in Food Sciences and Nutrition*, Vol.53, No. 3, 2013, pp. 251–275, https://10.1080/10408398.2010.518256.

[25] Versteeg, H.K. and Malalasekera, W., *An introduction to computational fluid dynamics: the finite volume method (2eds.)*, Pearson Education Limited, England, 2007.

[26] Assari, M.R., Basirat H. Tabrizi, and Saffar-Avval, M., Numerical simulation of fluid bed drying based on two-fluid model and experimental validation. *Applied Thermal Engineering*, Vol.27, No. 2-3, 2007, pp. 422–429, https://doi.org/10.1016/j.applthermaleng.2006.07.028.

[27] Verboven Pieter, de Baerdemaeker Josse and Nicolai M. Bart, Using computational fluid dynamics to optimise thermal processes. *Improving the Thermal Processing of Foods*, 2004, pp. 82–102, https://doi.org/10.1533/9781855739079.1.82.

[28] Christopher J. Greenshields, *The OpenFOAM foundation user guide version 11*, The OpenFOAM Foundation Ltd, London, United Kingdom, 2019, [Online]. https://openfoam.org (March 8, 2024).

[29] Bhusare, V.H., Dhiman, M.K., Kalaga, D.V., Roy, S. and Joshi, J.B., CFD simulations of a bubble column with and without internals by using OpenFOAM, *Chemical Engineering Journal*, Vol.317, 2017, pp. 157-174, https://doi.org/10.1016/j.cej.2017.01.128.

[30] Taguchi, G., *Taguchi on robust technology development methods*, ASME press, York, 1993, pp. 1-40.

Contribution of Individual Authors to the Creation of a Scientific Article (Ghostwriting Policy)

The authors equally contributed to the present research, at all stages from the formulation of the problem to the final findings and solution.

Sources of Funding for Research Presented in a Scientific Article or Scientific Article Itself

No funding was received for conducting this study.

Conflict of Interest

The authors have no conflicts of interest to declare.